Desalination and Water Treatment
www.deswater.com
doi: 10.1080/19443994.2015.1040854

57 (2016) 10560–10571
May

Taylor & Francis
Taylor & Francis Group

Biogenic silver nanocomposite TFC nanofiltration membrane with antifouling properties

Shasha Liu[a], Manying Zhang[a], Fang Fang[a], Li Cui[a], Junjie Wu[b], Robert Field[c], Kaisong Zhang[a,*]

[a]*Key Laboratory of Urban Pollutant Conversion, Institute of Urban Environment, Chinese Academy of Sciences, Xiamen 361021, China, Tel. +86 592 6190540; emails: ssliu@iue.ac.cn (S. Liu), myzhang@iue.ac.cn (M. Zhang), Tel. +86 592 6190534; emails: ffang@iue.ac.cn (F. Fang), lcui@iue.ac.cn (L. Cui), Tel./Fax: +86 592 6190782; email: kszhang@iue.ac.cn (K. Zhang)*
[b]*School of Engineering and Computing Sciences, Durham University, Durham DH1 3LE, UK, Tel. +44 191 33 42440; email: junjie.wu@durham.ac.uk*
[c]*Department of Engineering Sciences, University of Oxford, Oxford OX1 3PJ, UK, Tel. +44(0)1865 273814; email: robert.field@eng.ox.ac.uk*

Received 17 December 2014; Accepted 29 March 2015

ABSTRACT

Biofouling is still a major obstacle hindering wider application of thin-film composite (TFC) nanofiltration membranes in the water industry. One of the practical strategies to reduce biofouling is to develop novel antibiofouling membrane materials. Well-dispersed biogenic silver nanoparticles with a diameter of ~6 nm (Bio-Ag^0-6) were first immobilized in the selective layer of TFC nanofiltration membranes. Different dosages of Bio-Ag^0-6 were added in the aqueous solution during the interfacial polymerization of tetraethylenepentamine and 1,3,5-benzenetricarbonyl trichloride (TMC). Improved properties of Bio-Ag^0-6 /TFC membranes were systematically investigated. When the concentration of Bio-Ag^0-6 increased from 0 to 0.05 wt.% in aqueous solution, the water flux of TFC membranes increased from 7.31 to 13.76 $Lm^{-2}\,h^{-1}$ while maintaining the rejection of Na_2SO_4 at a relatively high level. The addition of Bio-Ag^0-6 also enhanced the hydrophilicity of Bio-Ag^0-6/TFC membranes in comparison with the bare TFC membranes. All Bio-Ag^0-6/TFC membranes exhibited an obvious antibacterial ability to inhibit the growth of *Pseudomonas aeruginosa*. Moreover, the Bio-Ag^0-6/TFC membranes showed the property of a low silver leaching rate in both the static immersion and the filtration systems. It demonstrated that the embedded Bio-Ag^0-6 in TFC membrane via interfacial polymerization improved the performance of the TFC nanofiltration membrane.

Keywords: Nanofiltration; Biogenic silver nanoparticles; Interfacial polymerization, antibacterial; Silver leaching rate

*Corresponding author.

1. Introduction

Membrane fouling is a major obstacle in thin-film composite (TFC) membrane application [1], since fouling causes various negative effects on membrane performance such as decreased permeate flux and increased energy and maintenance costs [2,3]. In terms of fouling components, fouling can be classified into three types: biofouling, organic fouling, and inorganic fouling [4]. Among them, biofouling is the most complicated, which drastically hinders the application of membrane processes [5]. Membrane biofouling is initiated by the adhesion of one of more bacteria to the membrane surface, followed by the growth and multiplication of the sessile cells, which can eventually develop a biofilm on the membrane surface [6]. Unlike physical or chemical fouling, biofouling is difficult to eliminate and causes irreversible damage to the membranes [7]. A common method to mitigate biofouling is feed water pretreatment. Physical pretreatments and chemical pretreatments are able to control scaling, inorganic, and parts of organic fouling. However, most antifouling measures by pretreatments are not effective in eliminating biofouling [8].

Recently, the combination of polymeric materials with nanoparticles has attracted much attention in TFC membrane fabrication. The addition of nanoparticles has introduced the concept of thin-film nanocomposite (TFN) membranes, which offer enhanced performance of membranes, such as reduced fouling, antimicrobial ability, and other new functionalities [9]. Lee et al. [10] fabricated TFC membranes with TiO_2 (~30 nm) nanoparticles in the selective layer through interfacial polymerization. Jin et al. [11] prepared polyamide (PA) thin-film NF membranes with nano-SiO_2 (~15 nm) by interfacial polymerization. The addition of SiO2 in the PA membrane improved the antifouling ability and increased the pure water flux without significant reduction of salt rejection. Lind et al. [12] prepared zeolite-polyamide TFN membranes by interfacial polymerization using particles of three sizes (100, 200, and 300 nm) added in the trimesoyl chloride (TMC) solution. The result demonstrated that smaller zeolites produced greater enhancement in membrane permeability. These nanoparticles can improve the antifouling ability of the TFC membranes.

Due to their excellent antibacterial properties and low toxicity to human cells [3,13,14], silver nanoparticles (AgNPs) have become an effective addition for fouling mitigation in polymeric membranes. Recently, efforts have been devoted to immobilize AgNPs into the selective layer of a membrane or grafted onto membrane surfaces. Lee et al. [15] added AgNPs in the oil phase to form a polyamine (PA) thin-film layer during the interfacial polymerization. Kim et al. [16] incorporated AgNPs into the MPD aqueous solution during the interfacial polymerization to improve antifouling properties of a TFC membrane. Yin et al. [17] attached AgNPs to the surface of PA TFC membrane effectively via covalent banding, with cysteamine as a bridging agent. These researches indicate that AgNPs can be immobilized to the TFC membrane via different methods and that positioning the AgNPs at the interface of a membrane allows for direct contact of AgNPs with bacterial cells for increased antimicrobial performance.

AgNPs in the aforementioned reports (diameter 15 ~ 100 nm) are all synthesized via chemical reduction. Chemically produced AgNPs often have problems in particle stability and tend to aggregate at high concentrations or when the average particle size is less than 40 nm. [18]. In addition, most physical and chemical methods are energy intensive or environmentally unfriendly, due to the use of toxic solvents or additives [19]. Hence, a more environment-friendly method, the biosynthesis of AgNPs, has been developed. Scientists have already tried to use biological materials for the synthesis of AgNPs. Bacteria, fungi, and some plant extracts are capable of producing AgNPs by reducing silver ions [20,21]. Some researchers have incorporated bio-Ag^0 into different casting solutions to fabricate ultrafiltration (UF) membranes [14,22]. These nanocomposite membranes showed improved antibacterial activity and could be applied to the treatment of drinking water. However, bio-Ag^0 is not yet known to be used in the fabrication of TFC nanofiltration membranes.

In our previous work, novel biogenic silver nanoparticles were reported using dried *Lactobacillus fermentum* biomass [23,24]. Biogenic silver nanoparticles with an average diameter of ~6 nm (Bio-Ag^0-6) showed high stability in aqueous solution. The attachment of the nanoparticles with the microscale surface of the bacterium on which they were formed prevents them from aggregating. The Bio-Ag^0-6 exhibited excellent antibacterial and antibiofouling performance in an UF membrane. The AgNPs acted via the direct interaction of the bacterial cells, the release of silver ions (Ag^+), and the generation of reactive oxygen species [25]. Morones et al. [26] indicated that the bactericidal properties of the nanoparticles were size-dependent, and nanoparticles that present a direct interaction with the bacteria preferentially have a diameter of approximately 1–10 nm. The size of Bio-Ag^0-6 is very small.

In this study, the antibiofouling characteristics of TFC nanofiltration membrane embedded with Bio-Ag^0-6 as antimicroble agent were investigated. The

effect of different contents of Bio-Ag^0-6 (0.005, 0.025, and 0.05 wt.%) on the permeate flux and antibiofouling properties was systematically investigated. The SEM, FT-IR, atomic force microscope (AFM), water contact angle measurements, and silver leaching test were also carried out to investigate the membrane surface morphology, its structure, and the stability of silver in the membrane. Furthermore, the flux and salt rejection of the Bio-Ag^0-6 contained TFC membranes after 4 months immersion experiment were tested, to evaluate whether the addition of Bio-Ag^0-6 in TFC membrane may influence the permeability of TFC membrane after part of the AgNPs release.

2. Experimental

2.1. Materials

Polysulfone (PS Solvay P3500) was bought from BASF (China) Co. Ltd. Polyvinylpyrrolidone (PVP-K30), triethylamine (TEA; ≥99%), sodium dodecyl sulfate (SDS; 99%), N-hexane (99%), sodium sulfate (Na_2SO_4), ammonia solution (analytical grade), and silver standard solution (1,000 mg L^{-1}) were supplied by Sinopharm Chemical Reagent Co., Ltd. N,N-dimethylacetamide (DMAc; ≥99%) was sourced from Jinshan Jingwei Chemical Co. Ltd, China. Silver nitrate ($AgNO_3$, analytical grade) was purchased from Shanghai Shenbo Chemical Co., Ltd. Tetraethylenepentamine (TEPA; 95%), and trimesoyl chloride (TMC; 98%) were purchased from Aladdin Co. Ltd.

2.2. Preparation of PS support membrane

The PS support membrane was prepared via the immersion precipitation phase inversion method. First, the blend solution was prepared by dissolving 18 wt.% PS in DMAc at 80˚C. After stirring for 12 h, the homogeneous solution was kept at room temperature to remove air bubbles for around 12 h. Then, the dope solution was cast onto a non-woven fabric (thickness of 100–110 μm) using a casting knife, followed by dipping the membrane into a deionized water bath for immediate phase inversion. The wet film thickness was controlled at ~200 μm. After 30 min in a gelation medium, the membrane was taken out and kept in 1 wt.% $NaHSO_3$ solution.

2.3. Synthesis and characterization of biogenic silver nanoparticles (Bio-Ag^0-6)

The biogenic silver nanoparticles (Bio-Ag^0-6) were synthesized with *L. fermentum* LMG 8900 as reported in a previous work [23]. The detailed procedure was as followed: dried biomass was dissolved into Milli-Q water in an Erlenmeyer flask, with NaOH and diamine silver added sequentially. The final concentration of biomass, silver, and $[OH]^{-1}$ was controlled to10, 10, and 0.2 mol L^{-1}, respectively. After incubating in a shaking incubator at 30˚C (200 rpm) for 24 h, the solution was centrifuged at 5,000 rpm for 6 min. The biogenic silver hydrosol was separated and centrifuged at 6,000 rpm for 10 min for further concentration and purification. The concentration of biogenic silver nanoparticles is 450 mg Ag g^{-1}, which is determined by inductively coupled plasma-optical emission spectrometer (ICP-OES).

2.4. Preparation of TFC NF membranes

The TFC NF membrane was prepared by interfacial polymerization of TEPA and TMC as described elsewhere [27,28]. The aqueous solutions were prepared according to the compositions given in Table 1, and stirred vigorously until completely dissolved. Firstly, the PS support layer was immersed in the aqueous phase for 10 min. The excess solution was removed from the soaked surface by an air knife. Then, the organic solution of TMC (0.5 wt.%) in n-hexane was poured over the membrane for 20 s to finish the interfacial polymerization reaction. The PS membrane was taken out from the n-hexane solution and heated in an oven at 40˚C for about 2 min, for a better polymerization reaction. Finally, the prepared TEPA/TMC composite nanofiltration membranes were rinsed and stored in distilled water.

2.5. Characterization of biogenic silver nanoparticles

To verify the reduction of silver ions, UV–visible analysis was carried out with a UV–vis spectrophotometer (DR5000 HACH) operating in the absorbance mode in the range of 200–600 nm. Distilled water was used as the blank. The size and morphology of the AgNPs were studied by transmission electron microscopy (TEM) (Tecnai F30). Size characterization of the samples was carried out on TEM images using Digital Micrograph software (Gatan Pleasanton, CA, USA). The data were statistically analyzed using SPSS 18.0 software (Armonk, NY, USA).

2.6. Membrane characterization

The surface morphologies of the composite membranes were observed by a field emission scanning electron microscope (FESEM, HITACHI S-4800) at an

Table 1
Composition of the aqueous solution with different bio-Ag^0-6

No.	TEPA (wt.%)	TEA (wt.%)	SDS (wt.%)	Bio-Ag^0-6 (wt.%)
M0	1	1	0.12	0
M1	1	1	0.12	0.005
M2	1	1	0.12	0.025
M3	1	1	0.12	0.05

accelerating voltage of 5 kV. Before SEM analysis, all membrane samples were dried in a vacuum oven at 80˚C for more than 48 h and coated with gold. Presence of silver nanoparticles was confirmed by energy dispersive X-ray spectra.

The functional groups of membrane surfaces were identified by ATR FT-IR spectroscopy, which was conducted on the Nicolet iS10 (Thermo Fisher Scientific) equipped with multi-reflection Smart Performer ATR accessory. All spectra included the wave numbers from 500 to 4,000 cm^{-1} with 64 scans at a resolution of 4.0 cm^{-1}.

The root mean square (RMS) roughness of the composite membranes was measured with an AFM MFP-3D (Asylum Research). Air-dried membrane samples were fixed on a specimen holder where 5 μm × 5 μm areas were scanned by a tapping node in the air. Three different images from each membrane sample were analyzed and their average values were taken as the final results.

Hydrophilicity of the membrane surface was assessed according to the pure water contact angle, which was measured by the sessile drop method on a video contact angle system (DSA100, German KRUSS). The contact angle was measured automatically by a video camera in the instrument using the drop shape analysis software. At least five measurements on different locations of each sample were performed to calculate an average value of contact angles.

The filtration performances of the composite membranes were evaluated by a dead-end filtration cell (Model 8,010, Millipore Corp. USA). The membranes (4.1 cm^2 of effective area) were operated at 25˚C and 0.35 MPa. Pure water flux was measured by the weight of permeate water at a constant transmembrane pressure. The weight of the permeate flux was recorded by a precision electronic balance (Denver Instrument, USA). 2000 ppm Na_2SO_4 was used as feeding solutions to test membrane rejection. The pure water flux and salt rejection were calculated with Eqs. (1) and (2), respectively.

$$J = \frac{W_p}{At} \tag{1}$$

$$R = \left(1 - \frac{C_p}{C_f}\right) \times 100\% \tag{2}$$

where J is the permeate flux ($Lm^{-2}\,h^{-1}$), W_p is the permeate volume (L), A is the membrane area (m^2), t is the filtration time (h), R is the rejection ratio, and C_p and C_f are the conductivities of permeate and feed solution, respectively. All the results presented are average data with standard deviation from at least three samples of each type of membrane.

2.7. Antibacterial assessment

Pseudomonas aeruginosa (ATCC27853) was inoculated into a liquid lysogeny broth and incubated in an incubator shaker (Zhicheng, ZHWY-2012C), shaking at 180 rpm for 10 h at 37˚C. The resulting cell suspension was further diluted to approximately 3×10^6 colony-forming units (CFU)/ml. Aliquots (100 μl) of the diluted working suspension inoculated with *P. aeruginosa* were applied to agar plates evenly. Membrane samples (diameter 2.1 cm) were then placed onto the nutrient agar plates with the selective layer in contact with the agar surface. After incubation at 37˚C for 24 h, the bacterial inhibition zone of each plate was observed. Furthermore, the membrane samples taken from the agar plates were dried in an oven at 80˚C for 24 h, and coated with platinum using a sputter coater for SEM observation.

2.8. Stability of the immobilized silver

The stability of the immobilized silver on the prepared composite nanofiltration membrane was evaluated via both static release and filtration experiments. In the static release test, the composite nanofiltration membrane was cut into a circular shape with an area of 3.6 cm^2, and was subsequently soaked in a sealed flask filled with 10 ml of Milli-Q water at room temperature. At specified time intervals, the water samples were collected and acidified by 2% HNO_3 to be analyzed by inductively coupled plasma mass spectrometry (ICP-MS, Agilent, model 7500CX).

The silver release rate under the filtration condition was evaluated by driving DI water through the membrane at a constant pressure of 0.35 MPa. The permeate water was collected every 1.5 h and released silver concentration measured by ICP-MS as described above.

To measure the silver content incorporated in the composite membrane, the membrane was digested by sonication in concentrated HNO_3 for 3 d. After digestion, the suspension was filtered to remove large particles and analyzed by ICP-MS for total silver content.

Further, the effect of silver depletion on the change of composite membranes filtration performance was also studied. First, the initial pure water flux and Na_2SO_4 rejection of the composite membranes were measured. Then, the membranes were immersed in 1% $NaHSO_3$ for 4 months, then 2% HNO_3 for 48 h, to maximize the release of silver. After that, the pure water flux and Na_2SO_4 rejection were tested again. Based on the data before and after immersion, the rates of flux and rejection variation can be calculated.

3. Results and discussion

3.1. Characterization of Bio-Ag^0-6

From the TEM image of Bio-Ag^0-6 in Fig. 1(a), it was found that biogenic silver nanoparticles were well dispersed and have a spherical morphology. The average diameter was about 6.1 nm, calculated by the software image J. The absorption spectra of TEPA aqueous solutions containing different amounts of Bio-Ag^0-6 were shown in Fig. 1(b). A well-defined peak centered at 420 nm was observed, corresponding to the plasmon excitation of AgNPs [15].

3.2. Characterization of the Bio-Ag^0-6 immobilized TFC membranes

The chemical structure of the selective layer was analyzed by ATR-FTIR spectroscopy, a convenient method to analyze the various chemical bonds in the outermost part of a membrane. The spectra for the PS support membrane and TFC membranes containing different concentrations of Bio-Ag^0-6 are presented in Fig. 2. Besides the typical PS bonds of the substrate, all spectra of TFC membranes M0, M1, M2, and M3 exhibited additional absorption peaks at 1,637 and 3,378 cm^{-1}, which were associated to C=O stretching vibration and N–H stretching vibration bands of amide groups [28]. These characteristic bands proved that the PA was formed on the surface of the PS substrate during the interfacial polymerization reaction. Compared to the spectrum of the bare composite NF membrane (M0), those of Bio-Ag^0-6/TFC membranes (M1, M2, and M3) were weaker. This may be attributed to two reasons: (i) the Bio-Ag^0-6 which covered on the surface of the composite membranes decreased the signals of the absorption peaks, and (ii) the extent of interfacial polymerization reaction was relatively reduced with the addition of Bio-Ag^0-6.

Images of TFC membranes containing different concentrations of Bio-Ag^0-6 are shown in Fig. 3(a). With the increased Bio-Ag^0-6 concentration in the

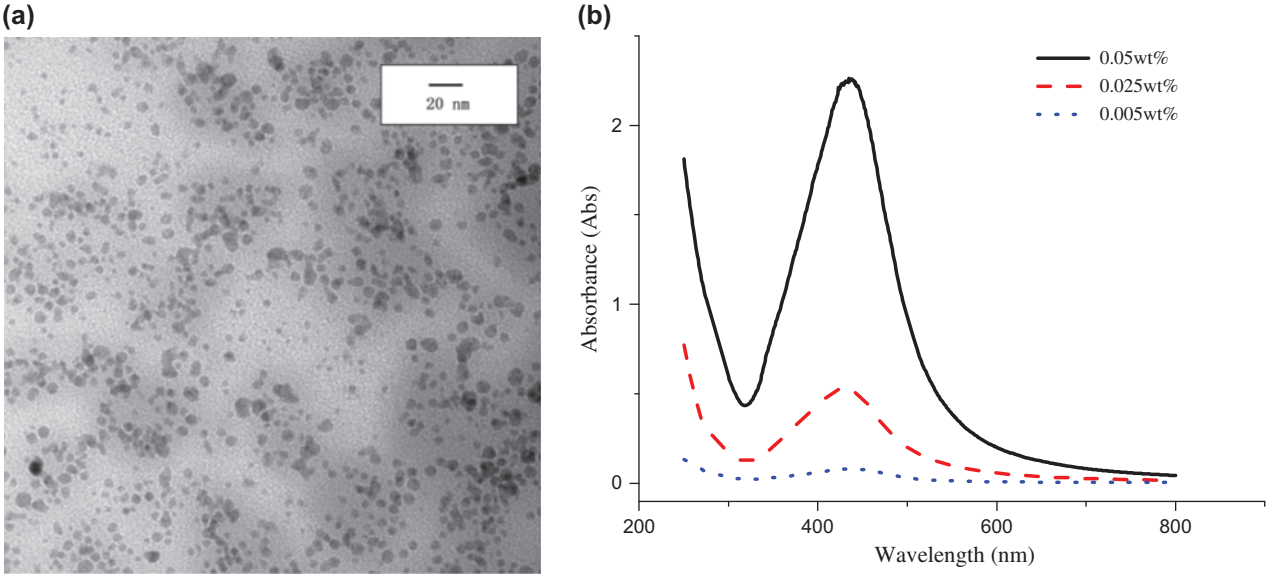

Fig. 1. TEM image of Bio-Ag^0-6 (a) and UV–vis absorption spectra of Bio-Ag^0-6 suspension (b).

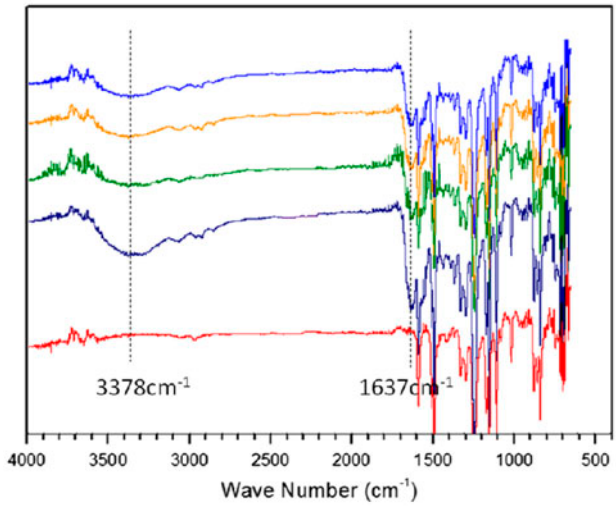

Fig. 2. FT-IR of PS substrate membrane and TFC membranes M0, M1, M2, and M3.

aqueous phase, the color of the composite membrane varied from white to tints of yellow, indicating that the immobilized amount of Bio-Ag^0-6 in the selective layer increased. Fig. 3(b) shows the surface morphologies of TFC membranes with different concentrations of Bio-Ag^0-6 added in the aqueous solution during the interfacial polymerization reaction. All of these membranes exhibited typical "ridge and valley" structure characteristic of the PA thin-film layer of TFC membrane [29]. Compared to the NF membrane without Bio-Ag^0-6 (M0), the membrane with 0.005% Bio-Ag^0-6 in aqueous solution (M1) has a relatively looser nodular structure. It is probably attributed to that the addition of hydrophilic Bio-Ag^0-6 enhanced the tension between the aqueous phase and oil phase and reduced the mass transfer of TEPA to organic phase. When the concentration of Bio-Ag^0-6 in aqueous solution increased to 0.05%, the ultra-thin layer surface became looser, which resulted in the increase in membrane permeability and decrease in the salt rejection. The

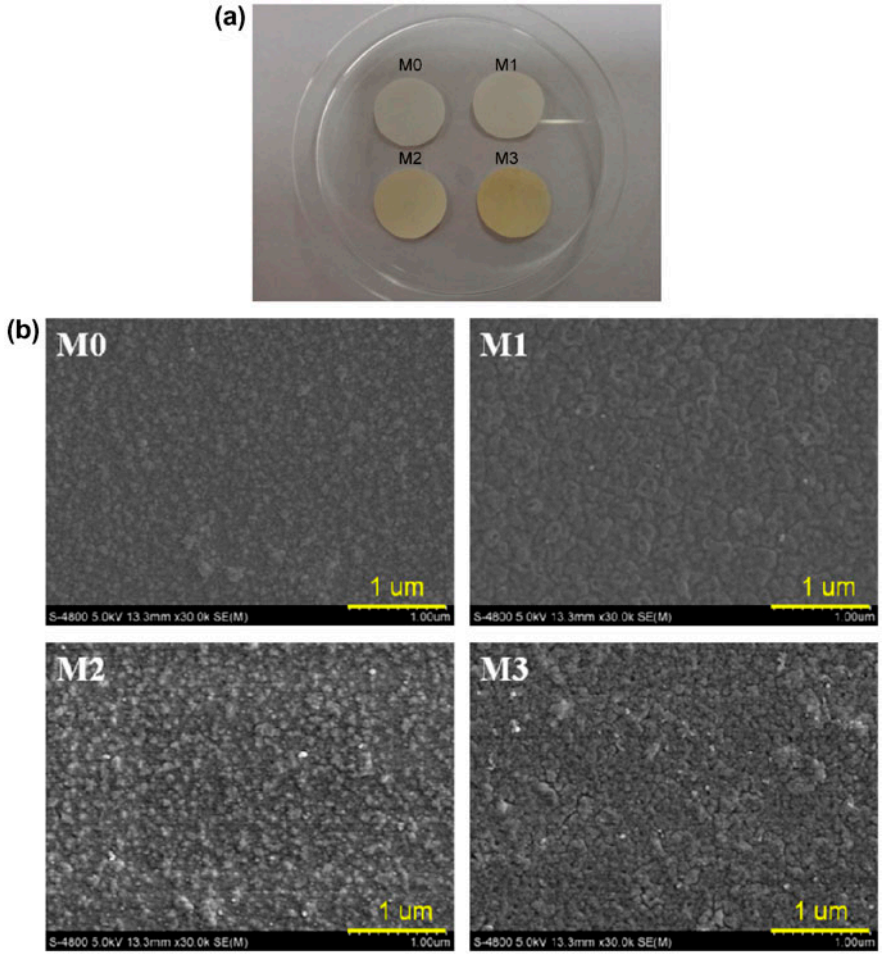

Fig. 3. (a) Images of TFC membrane samples and (b) SEM images of M0, M1, M2, and M3.

EDS spectra results (Table 2) indicated that the Bio-Ag^0-6 had successfully immobilized in the selective layer of the Bio-Ag^0-6/TFC membranes (M1, M2, and M3). As the Bio-Ag^0-6 content increased in the aqueous solution, the EDS spectra of Ag became stronger, especially for M3. Both the photos of the membranes and the EDS spectra proved that the content of AgNPs increased with the increased concentration of Bio-Ag^0-6 in aqueous solution during interface polymerization.

Fig. 4 presents AFM images of composite membranes (M0 and M1). A summary of the surface roughness values of the composite membranes is listed in Table 2. RMS height is a key physical parameter determined by AFM analysis; it is defined as the mean of the root for deviation from the standard surface to the indicated surface. High RMS means high surface roughness [30]. As shown in Fig. 4, the surfaces of the prepared TFC membranes (M0 and M1) exhibited abundant nodular structures, a well-known property of conventional interfacial polymerization for PA thin-film layers. The RMS of the composite NF membrane was reduced from 25.7 nm for the bare NF membrane (M0) to 10.9 nm for the Bio-Ag^0-6/TFC membrane (M1). This finding is consistent with the other results where the surface roughness experienced a decrease after the addition of AgNPs [13]. In general, all Bio-Ag^0-6/TFC membranes (M1, M2, and M3) had a smoother surface compared with the bare TFC membrane (M0). It is well established that the membrane with lower roughness and surface energy has stronger antifouling abilities [31,32].

Contact angles of TFC membranes (M0, M1, M2, and M3) were summarized in Table 2. The contact angle is a measure of tendency for water to wet the membrane surface. A lower contact angle means a better hydrophilicity of the membrane surface. It has been generally acknowledged that increasing membrane surface hydrophilicity could effectively reduce membrane fouling [33]. The contact angle gradually decreased from 41.8 to 33.0°when the Bio-Ag^0-6 concentration in the aqueous phase increased from 0 to 0.05 wt.%. The addition of Bio-Ag^0-6 had a great contribution to the surface hydrophilicity. This may attribute to the well-dispersed Bio-Ag^0-6 nanoparticles which contain a great deal of hydrophilic groups, such as hydroxyl groups and amino groups, responsible for the increase in hydrophilicity.

The main chemical components in the selective layer affecting the hydrophilicity of the membrane are amide groups, amino end groups (from the hydrolysis of unreacted acyl chloride groups), and AgNPs. The improved surface hydrophilicity of the TFC membrane prepared from a polymerization reaction of TEPA and TMC is mainly from the increased Bio-Ag^0-6 content at the surface skin layer.

3.3. Permeate flux and selectivity

The pure water permeability of the TFC membrane with different Bio-Ag^0-6 contents was determined by measuring the pure water flux through a dead-end filtration system. As presented in Table 3, with the increase in Bio-Ag^0-6 in aqueous solution, the pure water flux of the TFC membranes increased from 7.31 to 13.76 L/m^2 h at 0.35 MPa. The presence of Bio-Ag^0-6 in the aqueous solution during the interfacial polymerization reaction can effectively enhance the water permeability compared with the bare TFC membrane. The pure water flux of the Bio-Ag^0-6/TFC membrane with AgNPs was higher than that of the bare TFC membrane.

The rejection rate of the TFC membrane to salt is mainly determined by both the size and Donnan exclusion effects [34]. In Table 3, when the concentrations of Bio-Ag^0-6 increased from 0 to 0.025 wt.% in the aqueous solution, the salt rejection of the prepared Bio-Ag^0-6/TFC membranes slightly decreased from 88.46 to 86.71%. When the concentration of Bio-Ag^0-6 reached 0.05 wt.%, the rejection decreased drastically to 68.33%. This may be due to the high concentration of Bio-Ag^0-6 in aqueous phase blocking the degree of TEPA/TMC chemical cross-linking, resulting in a loose membrane structure, which will increase the pore size and weaken the size exclusion effect. The results were consistent with the SEM images.

Table 2
Surface elemental composition of M0, M1, M2, and M3

	Element				
Membrane samples	Ag (%)	C (%)	O (%)	S (%)	Au (%)
M0	0	3.18	1.14	8.82	86.86
M1	0.25	2.72	0.63	7.64	88.76
M2	1.63	2.62	0.78	7.67	87.30
M3	2.71	2.17	1.08	7.27	86.24

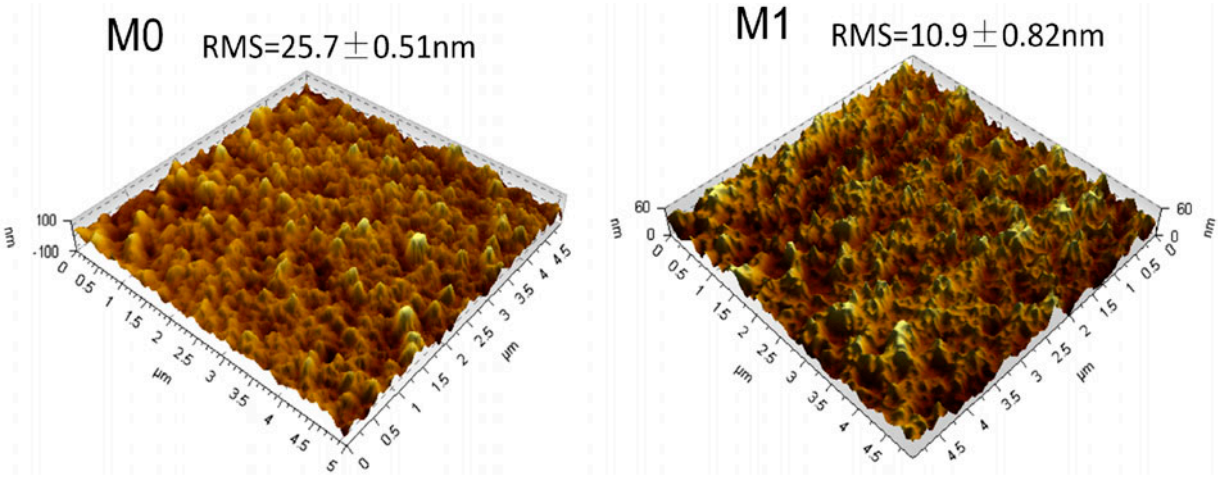

Fig. 4. AFM images of bare TFC membrane (M0) and nanocomposite TFC membrane (M1).

Table 3
Roughness, contact angle, pure water flux, and salt rejection of the prepared TFC membranes

Membrane	Roughness (nm)	Contact angle (°)	Water flux (L/m^2 h)	Rejection of Na_2SO_4 (%)
M0	25.7 ± 0.51	41.8 ± 0.94	7.31 ± 2.7	88.46 ± 2.2
M1	10.9 ± 0.82	38.6 ± 1.28	9.88 ± 0.5	87.95 ± 2.2
M2	8.05 ± 4.31	37.8 ± 0.94	10.34 ± 0.1	86.71 ± 2.5
M3	20.3 ± 0.57	33.0 ± 0.91	13.76 ± 3.0	68.33 ± 1.3

Note: (2,000 ppm Na_2SO_4, 0.35 MPa).

3.4. Antibacterial tests

P. aeruginosa was chosen as the test bacteria in the disk diffusion test. The results shown in Fig. 5 indicated that the prepared Bio-Ag^0-6/TFC membranes had a significant inhibition capacity to the *P. aeruginosa*. The bare TFC membrane did not show any inhibition effect toward the growth of *P. aeruginosa*. With the increase in Bio-Ag^0-6 content, the inhibition zone became clearer and larger. Although there was no obvious inhibition zone around membrane M1, the amount of *P. aeruginosa* attached to the surface of the membrane decreased evidently. Both M2 and M3 had a clear bacterial inhibition zone.

Fig. 6 shows the SEM images of bacteria grown on different types of membranes taken from the disk diffusion experiment. It can be observed that the surface of the bare TFC membrane (M0) was covered with a dense layer of bacteria. The results for the Bio-Ag^0-6/TFC membranes were quite different from that of bare TFC membrane. Less bacteria were observed on the membrane surface and the membranes with higher silver loading (M2 and M3) seemed nearly free of bacterial growth. The results may be attributed to the higher hydrophilicity, the lower roughness, and the bactericidal effects of AgNPs [35,36].

Some researches explained that the antibacterial capacity of silver composite membranes mainly relies on their ability to release silver ions (Ag^+), which has a strong toxicity to bacteria. Silver ions can react with cysteine by replacing the hydrogen atom of the thiol group to form S–Ag complexes [37], thus might altering protein structure and hindering enzyme action, particularly respiratory function. Furthermore, Ag^+ can influence the structure and the permeability of the cell membrane [38,39].

The above results clearly indicate that the incorporation of Bio-Ag^0-6 can effectively enhance the antibacterial performance of the TFC membranes.

3.5. Analysis of silver leaching

The release rate of silver from the selective layer of the TFC membrane was examined in both static and filtration experiments. As presented in Fig. 7, the initial silver ions released from M1, M2, and M3 were 0.013, 0.16, and 0.20 μg cm^{-2} d^{-1}, respectively, which

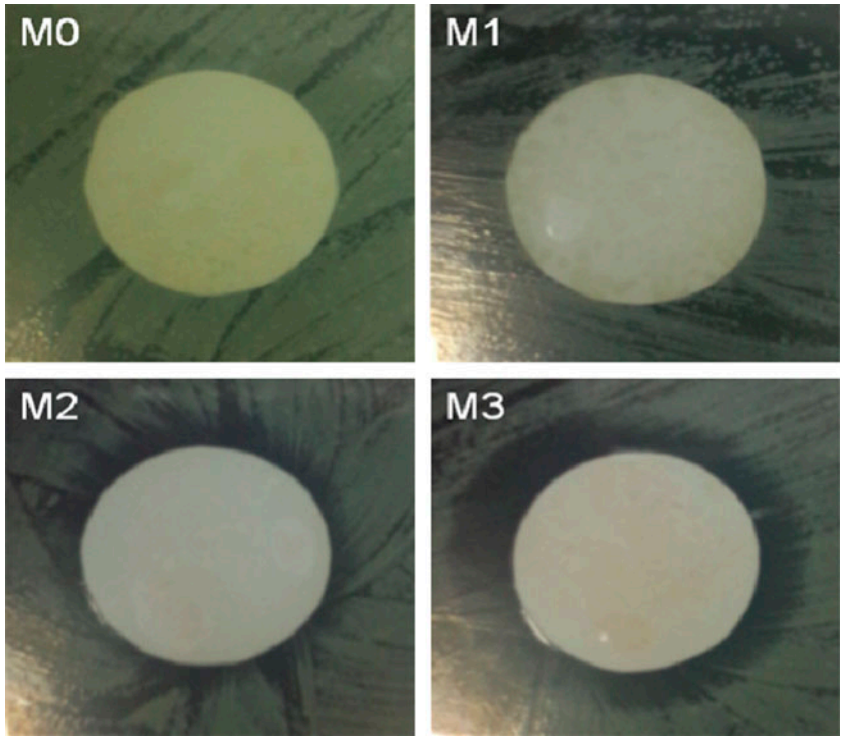

Fig. 5. Inhibition zone for *P. aeruginosa* (PA) on composite NF membranes M0, M1, M2, and M3.

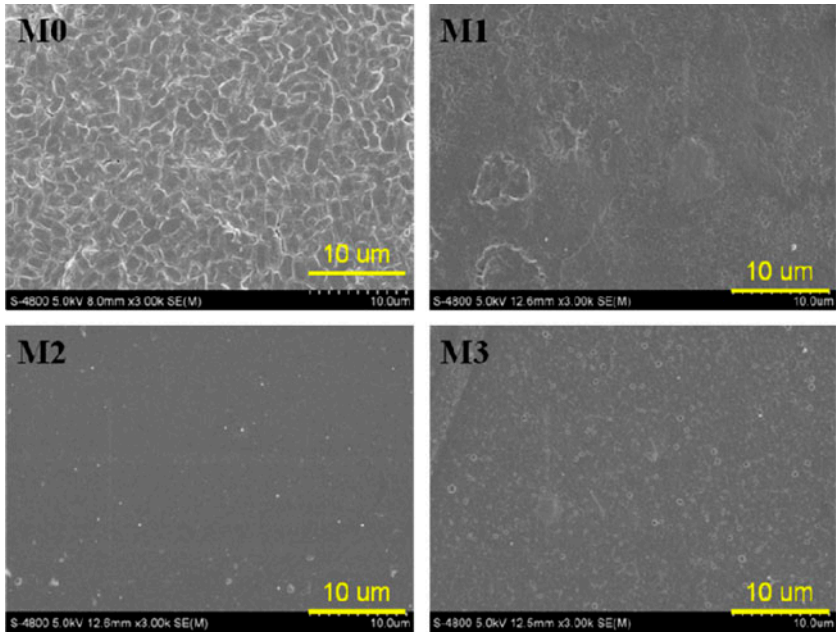

Fig. 6. SEM images of TFC membranes M0, M1, M2, and M3 after batch incubation with *P. aeruginosa* (PA) at 37°C for 24 h.

then declined steadily with time. The release rate of M1, M2, and M3 leveled off to a level below 0.01 μg cm^{-2} d^{-1} after being soaked in Milli-Q water for 40 d. The total amount of Bio-Ag^0-6 immobilized in the selective layer of TFC membranes M1, M2, and M3 were 1.05, 3.61, and 4.96 μg cm^{-2}, respectively. After 40 d of the static release test, the ratio of the remaining silver to the original amount in the Bio-Ag^0-6/TFC membranes was 97, 89, and 75% for M1, M2, and M3, respectively. Due to the relatively low leaching rate of around 0.01 μg cm^{-2} d^{-1}, all the membranes are expected to last more than 5 months until all the silver in the membranes is completely released. This will potentially extend the life of the antifouling effect of the TFC membrane.

The concentration of silver ions in the permeate fluid during filtration was analyzed by ICP-MS. The result is presented in Fig. 8. For all the tested membranes, Ag^+ leaching increased at a higher Bio-Ag^0-6 content. The leaching Ag^+ concentration in the permeate side was very low with an initial concentration being less than 25 ppb for M3, and less than 5 ppb for M1 and M2. The release rate of Ag^+ gradually decreased as more water was filtered with time. According to the National Secondary Drinking Water Regulations, the Ag threshold is limited to 100 ppb. Hence, the amount of silver released from the prepared Bio-Ag^0-6/TFC membranes (M1, M2, and M3) has no health concern. According to the filtration experiment, the prepared TFC membranes with Bio-Ag^0-6 could be a good choice for membrane biofouling disinfection since the Ag^+ release was below the threshold value during the filtration process. The leaching results suggested that the antimicrobial effect of Bio-Ag^0-6 could last for a long time.

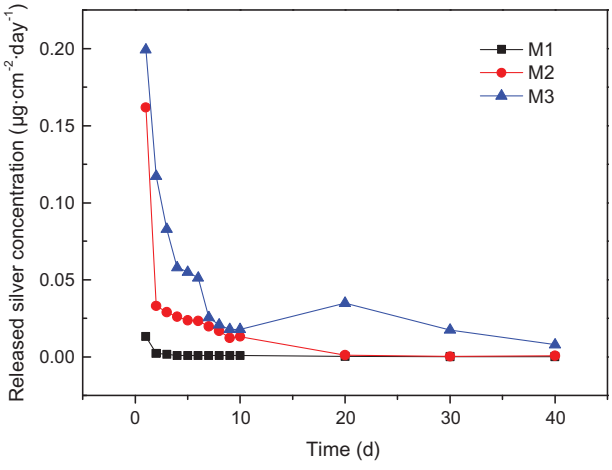

Fig. 7. The release rate of silver during 40 d leaching test.

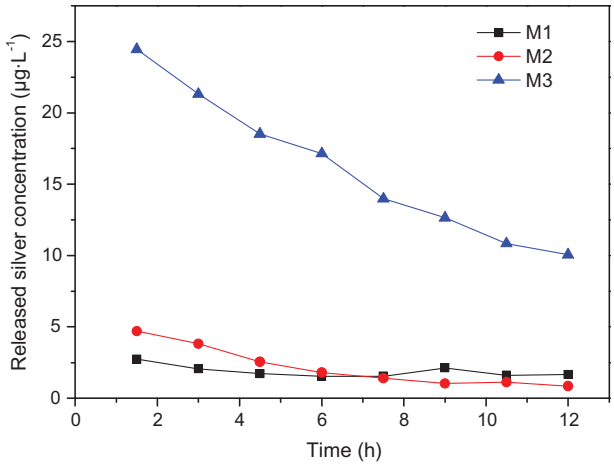

Fig. 8. Concentration of leached silver in the solutions filtered by the test membranes M1, M2, and M3.

Although the antibacterial action by AgNPs is not fully studied, several researchers inferred that the antibacterial capacity of the composite membranes is based on their ability to release biotoxic silver ions (Ag^+) into the surrounding solution [40]. Several studies have proved that the antibacterial capacity of silver-loaded membranes had a significant reduction due to a decrease in the silver content [41]. In this study, after 40 d of soaking process, most of the silver remained inside the membranes.

As shown in Fig. 9, the Bio-Ag^0-6/TFC membranes (M1 and M2) show an excellent stability of flux and selectivity. After the membranes soaked in $NaHSO_3$ for 4 months and in 2% HNO_3 for 48 h, the Na_2SO_4 rejection of bare TFC membrane (M0) is 74.08%, only 88% compared with the initial rejection of M0. While the Na_2SO_4 rejections of Bio-Ag^0-6/TFC (M1 and M2) were

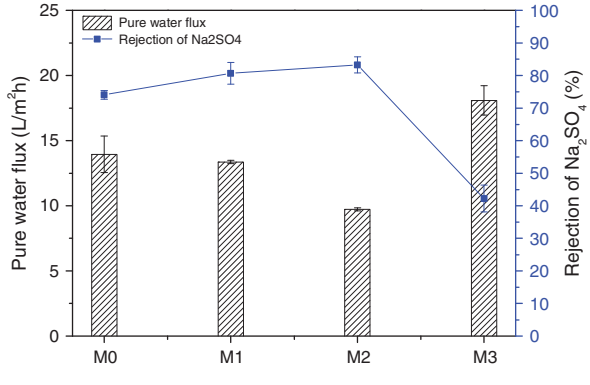

Fig. 9. The pure water flux and salt rejection of M0, M1, M2, and M3 after silver depletion treatment (soaked in 1% $NaHSO_3$ for 4 months and 2% HNO_3 for 48 h).

80.63% and 83.25%, respectively. The rejections of M1 and M2 were more than 91% compared with the initial rejection of M1 and M2. The result indicated that the Bio-Ag^0-6 nanoparticles may have a strong binding strength with the PA polymer and could be held tightly in the selective layer which is consistent with the results of the silver leaching during 12-h filtration. The release of silver from the membrane may form the outer surface of the selective layer of the TFC membrane. So, it is expected that a kind of stable and novel antibiofouling TFC nanofiltration membrane could be achieved.

4. Conclusions

The improved properties of the TFC nanofiltration membranes were achieved by adding Bio-Ag^0-6 in aqueous solution during interfacial polymerization. The following conclusions can be drawn from the experimental results.

(1) The Bio-Ag^0-6 was successfully introduced in the selective layer of the TFC membranes. Bio-Ag^0-6 enhanced the hydrophilicity and decreased the surface roughness value of the TFC membranes, which may reduce the attachment of microbes.
(2) The addition of Bio-Ag^0-6 can improve the permeability of the TFC membrane. Both membranes M1 and M2 showed higher pure water flux compared to the bare TFC membrane (M0) while maintaining a high rejection to Na_2SO_4.
(3) In terms of bacterial analysis, the Bio-Ag^0-6/TFC membranes exhibited excellent antibiofouling performance. The results demonstrated that the Bio-Ag^0-6 nanoparticles in the TFC membranes could be an effective approach to reduce membrane biofouling.
(4) The released silver from the Bio-Ag^0-6/TFC membranes was in the safe range and had less influence on the filtration performance compared to the bare TFC membrane, indicating the stability of immobilized silver in the membranes.

Acknowledgments

KSZ thanks Royal Academy of Engineering, UK, for the Research Exchange with China/India scheme. The authors gratefully acknowledge the financial support of Xiamen Municipal Bureau of Science and Technology (3502Z20131159). The authors are also grateful to Dr Steve Chapman from The James Hutton Institute for polishing the manuscript and insightful comments.

References

[1] E. Bar-Zeev, I. Berman-Frank, B. Liberman, E. Rahav, U. Passow, T. Berman, Transparent exopolymer particles: Potential agents for organic fouling and biofilm formation in desalination and water treatment plants, Desalin. Water Treat. 3 (2009) 136–142.
[2] H. Wu, B. Tang, P. Wu, Preparation and characterization of anti-fouling β-cyclodextrin/polyester thin film nanofiltration composite membrane, J. Membr. Sci. 428 (2013) 301–308.
[3] A. Dror-Ehre, A. Adin, H. Mamane, Control of membrane biofouling by silver nanoparticles using *Pseudomonas aeruginosa* as a model bacterium, Desalin. Water Treat. 48 (2012) 130–137.
[4] S. Kappachery, D. Paul, J. Yoon, J.H. Kweon, Vanillin, a potential agent to prevent biofouling of reverse osmosis membrane, Biofouling 26 (2010) 667–672.
[5] H.-L. Yang, J.C.-T. Lin, C. Huang, Application of nanosilver surface modification to RO membrane and spacer for mitigating biofouling in seawater desalination, Water Res. 43 (2009) 3777–3786.
[6] N. Hilal, V. Kochkodan, L. Al-Khatib, T. Levadna, Surface modified polymeric membranes to reduce (bio)-fouling: A microbiological study using *E. coli*, Desalination 167 (2004) 293–300.
[7] C.X. Liu, D.R. Zhang, Y. He, X.S. Zhao, R. Bai, Modification of membrane surface for anti-biofouling performance: Effect of anti-adhesion and anti-bacteria approaches, J. Membr. Sci. 346 (2010) 121–130.
[8] T. Kim, Y. Kim, Y. Choi, J. Kweon, J. Song, N. Gang, Biofilm formation and its effect on biofouling in RO membrane processes for wastewater reuse, Desalin. Water Treat. 2 (2009) 71–75.
[9] M.M. Pendergast, E.M.V. Hoek, A review of water treatment membrane nanotechnologies, Energy Environ. Sci. 4 (2011) 1946.
[10] H.S. Lee, S.J. Im, J.H. Kim, H.J. Kim, J.P. Kim, B.R. Min, Polyamide thin-film nanofiltration membranes containing TiO_2 nanoparticles, Desalination 219 (2008) 48–56.
[11] L. Jin, W. Shi, S. Yu, X. Yi, N. Sun, C. Ma, Y. Liu, Preparation and characterization of a novel PA-SiO2 nanofiltration membrane for raw water treatment, Desalination 298 (2012) 34–41.
[12] M.L. Lind, A.K. Ghosh, A. Jawor, X. Huang, W. Hou, Y. Yang, E.M. Hoek, Influence of zeolite crystal size on zeolite-polyamide thin film nanocomposite membranes, Langmuir 25 (2009) 10139–10145.
[13] J. Huang, H.T. Wang, K.S. Zhang, Modification of PES membrane with Ag–SiO_2: Reduction of biofouling and improvement of filtration performance, Desalination 336 (2014) 8–17.
[14] M. Zhang, K. Zhang, B. De Gusseme, W. Verstraete, Biogenic silver nanoparticles (bio-Ag^0) decrease biofouling of bio-Ag^0/PES nanocomposite membranes, Water Res. 46 (2012) 2077–2087.
[15] S.Y. Lee, H.J. Kim, R. Patel, S.J. Im, J.H. Kim, B.R. Min, Silver nanoparticles immobilized on thin film composite polyamide membrane: Characterization, nanofiltration, antifouling properties, Polym. Adv. Technol. 18 (2007) 562–568.
[16] E.-S. Kim, G. Hwang, M. Gamal El-Din, Y. Liu, Development of nanosilver and multi-walled carbon

nanotubes thin-film nanocomposite membrane for enhanced water treatment, J. Membr. Sci. 394–395 (2012) 37–48.
[17] J. Yin, Y. Yang, Z. Hu, B. Deng, Attachment of silver nanoparticles (AgNPs) onto thin-film composite (TFC) membranes through covalent bonding to reduce membrane biofouling, J. Membr. Sci. 441 (2013) 73–82.
[18] F. Mafuné, J.-Y. Kohno, Y. Takeda, T. Kondow, H. Sawabe, Structure and stability of silver nanoparticles in aqueous solution produced by laser ablation, J. Phys. Chem. B 104 (2000) 8333–8337.
[19] J. Huang, G. Arthanareeswaran, K. Zhang, Effect of silver loaded sodium zirconium phosphate (nanoAgZ) nanoparticles incorporation on PES membrane performance, Desalination 285 (2012) 100–107.
[20] R.S. Patil, M.R. Kokate, S.S. Kolekar, Bioinspired synthesis of highly stabilized silver nanoparticles using *Ocimum tenuiflorum* leaf extract and their antibacterial activity, Spectrochim. Acta, Part A 91 (2012) 234–238.
[21] V.K. Sharma, R.A. Yngard, Y. Lin, Silver nanoparticles: Green synthesis and their antimicrobial activities, Adv. Colloid Interface Sci. 145 (2009) 83–96.
[22] B. De Gusseme, T. Hennebel, E. Christiaens, H. Saveyn, K. Verbeken, J.P. Fitts, N. Boon, W. Verstraete, Virus disinfection in water by biogenic silver immobilized in polyvinylidene fluoride membranes, Water Res. 45 (2011) 1856–1864.
[23] M. Zhang, K. Zhang, B. De Gusseme, W. Verstraete, R. Field, The antibacterial and anti-biofouling performance of biogenic silver nanoparticles by *Lactobacillus fermentum*, Biofouling 30 (2014) 347–357.
[24] M. Zhang, R. Field, K. Zhang, Biogenic silver nanocomposite polyethersulfone UF membranes with antifouling properties, J. Membr. Sci. 471 (2014) 274–284.
[25] Q. Bao, D. Zhang, P. Qi, Synthesis and characterization of silver nanoparticle and graphene oxide nanosheet composites as a bactericidal agent for water disinfection, J. Colloid Interface Sci. 360 (2011) 463–470.
[26] J.R. Morones, J.L. Elechiguerra, A. Camacho, K. Holt, J.B. Kouri, J.T. Ramírez, M.J. Yacaman, The bactericidal effect of silver nanoparticles, Nanotechnology 16 (2005) 2346–2353.
[27] X. Fan, Y. Dong, Y. Su, X. Zhao, Y. Li, J. Liu, Z. Jiang, Improved performance of composite nanofiltration membranes by adding calcium chloride in aqueous phase during interfacial polymerization process, J. Membr. Sci. 452 (2014) 90–96.
[28] Y. Li, Y. Su, Y. Dong, X. Zhao, Z. Jiang, R. Zhang, J. Zhao, Separation performance of thin-film composite nanofiltration membrane through interfacial polymerization using different amine monomers, Desalination 333 (2014) 59–65.
[29] J. Xiang, Z. Xie, M. Hoang, D. Ng, K. Zhang, Effect of ammonium salts on the properties of poly(piperazineamide) thin film composite nanofiltration membrane, J. Membr. Sci. 465 (2014) 34–40.
[30] L. Li, S. Zhang, X. Zhang, Preparation and characterization of poly(piperazineamide) composite nanofiltration membrane by interfacial polymerization of 3,3′,5,5′-biphenyl tetraacyl chloride and piperazine, J. Membr. Sci. 335 (2009) 133–139.
[31] A. Razmjou, J. Mansouri, V. Chen, The effects of mechanical and chemical modification of TiO_2 nanoparticles on the surface chemistry, structure and fouling performance of PES ultrafiltration membranes, J. Membr. Sci. 378 (2011) 73–84.
[32] Y. Chen, Y. Zhang, H. Zhang, J. Liu, C. Song, Biofouling control of halloysite nanotubes-decorated polyethersulfone ultrafiltration membrane modified with chitosan-silver nanoparticles, Chem. Eng. J. 228 (2013) 12–20.
[33] H. Yu, Y. Zhang, J. Zhang, H. Zhang, J. Liu, Preparation and antibacterial property of SiO_2–Ag/PES hybrid ultrafiltration membranes, Desalin. Water Treat. 51 (2013) 3584–3590.
[34] S. Yu, Q. Zhou, S. Shuai, G. Yao, M. Ma, C. Gao, Thin-film composite nanofiltration membranes with improved acid stability prepared from naphthalene-1,3,6-trisulfonylchloride (NTSC) and trimesoyl chloride (TMC), Desalination 315 (2013) 164–172.
[35] Y. Xiong, Y. Liu, Biological control of microbial attachment: A promising alternative for mitigating membrane biofouling, Appl. Microbiol. Biotechnol. 86 (2010) 825–837.
[36] P. Landini, D. Antoniani, J.G. Burgess, R. Nijland, Molecular mechanisms of compounds affecting bacterial biofilm formation and dispersal, Appl. Microbiol. Biotechnol. 86 (2010) 813–823.
[37] H. Basri, A. Ismail, M. Aziz, Polyethersulfone (PES)–silver composite UF membrane: Effect of silver loading and PVP molecular weight on membrane morphology and antibacterial activity, Desalination 273 (2011) 72–80.
[38] L. Cui, P. Chen, S. Chen, Z. Yuan, C. Yu, B. Ren, K. Zhang, *In Situ* study of the antibacterial activity and mechanism of action of silver nanoparticles by surface-enhanced Raman spectroscopy, Anal. Chem. 85 (2013) 5436–5443.
[39] Q. Feng, J. Wu, G. Chen, F. Cui, T. Kim, J. Kim, A mechanistic study of the antibacterial effect of silver ions on *Escherichia coli* and *Staphylococcus aureus*, J. Biomed. Mater. Res. 52 (2000) 662–668.
[40] X. Cao, M. Tang, F. Liu, Y. Nie, C. Zhao, Immobilization of silver nanoparticles onto sulfonated polyethersulfone membranes as antibacterial materials, Colloid. Surf., B 81 (2010) 555–562.
[41] W.L. Chou, D.G. Yu, M.C. Yang, The preparation and characterization of silver-loading cellulose acetate hollow fiber membrane for water treatment, Polym. Adv. Technol. 16 (2005) 600–607.